Published in Electrochimica Acta 53, issue 5, 2210-2216, 2008
which should be used for any reference to this work

Improvement of the structural and chemical properties of a commercial activated carbon for its application in electrochemical capacitors

G. Lota [a], T.A. Centeno [b,*], E. Frackowiak [a], F. Stoeckli [c]

[a] *Poznan University of Technology, Institute of Chemistry and Technical Electrochemistry, Piotrowo 3, 60-965 Poznan, Poland*
[b] *Instituto Nacional del Carbón-C.S.I.C. Apartado 73, 33080 Oviedo, Spain*
[c] *IMT-Chimie des Surfaces, Université de Neuchâtel. Rue Emile Argand 11, CH-2009 Neuchâtel, Switzerland*

Abstract

The present paper shows that the performance of an inexpensive activated carbon used in electrochemical capacitors can be significantly enhanced by a simple treatment with KOH at 850 °C. The changes in the specific surface area, as well as in the surface chemistry, lead to high capacitance values, which provide a noticeable energy density.

The KOH-treatment of a commercial activated carbon leads to highly pure carbons with effective surface areas in the range of 1300–1500 $m^2\,g^{-1}$ and gravimetric capacitances as high as three times that of the raw carbon.

For re-activated carbons, one obtains at low current density (50 $mA\,g^{-1}$) values of 200 $F\,g^{-1}$ in aqueous electrolytes (1M H_2SO_4 and 6M KOH) and around 150 $F\,g^{-1}$ in 1M $(C_2H_5)_4NBF_4$ in acetonitrile. Furthermore, the resulting carbons present an enhanced and stable performance for high charge/discharge load in organic and aqueous media.

This work confirms the possibilities offered by immersion calorimetry on its own for the prediction of the specific capacitance of carbons in $(C_2H_5)_4NBF_4$/acetonitrile. On the other hand, it also shows the limitations of this technique to assess, with a good accuracy, the suitability of a carbon to be used as capacitor electrodes operating in aqueous electrolytes (H_2SO_4 and KOH).

Keywords: Carbon; Porosity; Pore size distribution; Immersion calorimetry; Electrochemical capacitor

1. Introduction

Electrochemical capacitors, also called supercapacitors or ultracapacitors, are currently a topic of active research in view of the limitations of conventional electrical systems to provide high power-energy density for novel applications. In recent years, these devices have been extensively used in power distribution systems, electronic devices, uninterrupted power supplies, electric vehicles, etc. [1–3].

At the present time, most commercial electrochemical capacitors correspond to those referred to as electrochemical double layer capacitors (EDLCs). The double layer is established when an electronic conductor is in contact with an ionic conductor: a charge separation takes place on either side of the interface leading to the formation of an electrochemical double layer. The current generated during this process is essentially due to the rearrangement of charges when a voltage is applied. No charge transfer from chemical reactions in the electrode takes place. The EDLC mechanism requires electrodes made of materials with high specific surface area, a requirement for high charge accumulation and a suitable pore structure to allow a rapid motion of the electrolyte ions [1–3].

A large variety of carbonaceous materials such as activated carbons (powders or fibers), carbon aerogels/xerogels, carbon nanotubes, templated mesoporous carbons, etc., have been extensively studied as electrodes in EDLCs, most of them presenting very promising properties [4]. However, economic analyses indicate that a key issue for the implementation of electrochemical capacitors in a large volume market is the unit cost of the carbon in relation to its specific capacitance [3]. As far as activated carbons are concerned, the potentiality is high and many efforts are devoted to the improvement of their physicochemical properties, in order to optimize their performances in supercapacitors.

* Corresponding author. Tel.: +34 985119090; fax: +34 985297662.
E-mail address: teresa@incar.csic.es (T.A. Centeno).

Recent studies have identified some key parameters of carbons for high capacitance and high voltage devices [5–10]. Firstly, it has been shown that for the aqueous H_2SO_4 electrolyte the specific capacitance of activated carbons at low current densities consists of a contribution from the total accessible surface area and of an additional pseudo-capacitance based on quick faradaic reactions. The latter arise from certain surface functionalities, such as species generating CO in thermally programmed desorption (TPD) [5–8] and nitrogen-containing groups [9]. Secondly, the pseudo-capacitive effects in the aprotic electrolyte $(C_2H_5)_4NBF_4$ in acetonitrile seem to be much weaker than in the aqueous electrolyte and the performance of the corresponding supercapacitors results basically from an EDLC mechanism [10].

Furthermore, it appears that the variation of the specific capacitance at high current densities in the aqueous H_2SO_4 electrolyte is controlled by the average micropore width (L_o) and the amount of CO_2 generating surface groups [8]. The influence of L_o is perceptible for activated carbons with low oxygen contents, but for oxidized materials the CO_2-generating functionalities have a predominant effect on the reduction of the capacitance. On the other hand, since the capacitances in the aprotic and the acidic electrolytes decrease in a similar fashion for the individual carbons, it has been suggested that the same mechanism applies in both media with a scaling factor [10]. Although further studies are required, these approaches provide a useful insight into the pathway for the optimization of carbons to be used in supercapacitors.

The present paper shows that the electrochemical capacitor performance of an inexpensive activated carbon can be notably enhanced by a secondary activation with KOH at 850 °C. The resulting changes in the porous structure, as well as in the chemical features of the carbon surface, improve the performances for high power applications.

2. Experimental

2.1. Carbons

A commercial activated carbon, Norit® SX2 POCH-Poland, was used as raw material (this carbon is hereafter labelled N0). Samples N1–N4 resulted from the treatment of N0 by KOH to weight losses (burn-off) around 30 and 50%. The treatment conditions are summarized in Table 1.

The resulting carbons were rinsed with hot distilled water and subsequently treated with 10% HCl. Finally, the solids were washed with distilled water until no chloride was detected (test with Ag^+) and dried in air at around 110 °C.

For comparison, data for other porous carbons determined under similar experimental conditions are also included in the present work [7–11].

2.2. Chemical characteristics of carbons

The carbon, hydrogen, nitrogen and sulfur contents of the samples were determined using a LECO-CHNS-932 elemental analyzer. The oxygen content was determined directly using a LECO-VTF-900 graphite furnace. The results, including the ash contents, are shown in Table 1.

2.3. Analysis of the porous structure of the carbons

The solids have been well characterized by different and converging techniques such as N_2 adsorption at 77 K (*Micromeritics ASAP 2010*) and immersion calorimetry at 293 K. The latter is based on the use of liquid probes having different molecular sizes (dichloromethane (0.33 nm), benzene (0.41 nm), cyclohexane (0.54 nm), carbon tetrachloride (0.63 nm), cyclododeca-1,5,9-triene CDDT (0.76 nm), tri-2,4-xylylphosphate TXP (1.50 nm)) and aqueous solution 0.4M of phenol. These techniques have been described in detail elsewhere [12–14].

The theoretical background for microporosity characterization is provided by Dubinin's theory and its extension to immersion calorimetry [12,13]. The data was further cross-checked by a classical comparison plot based on the N_2 adsorption on the given carbon and on a non-porous reference, *Vulcan 3G*. The initial linear section of the plot reflects the total surface area of the solid under investigation whereas the final linear section corresponds to the external surface area S_e [14].

The foregoing techniques lead therefore to reliable values of the micropore volume W_o, the average micropore dimension L_o, the micropore size distribution, the microporous surface area S_{mi} and the external (non-microporous) surface S_e. The total surface area was also estimated from the enthalpy of immersion into aqueous solution of phenol. The corresponding values are given in Table 2.

2.4. Electrochemical characterization

Two-electrode capacitors were assembled in a Swagelok® system with pellets of comparable mass. The electrode was composed of 85 wt.% of carbon, 10 wt.% of polivinylidene fluoride

Table 1
Experimental conditions of KOH-treatment of carbon N0 at 850 °C and chemical characteristics of the resulting carbons

Carbon	KOH reactivation			Chemical characteristics				
	Ratio N0:KOH	Activation time (h)	Burn-off (%)	C (% wt)	O (% wt)	N (% wt)	H (% wt)	Ash (% wt)
N0	–	–	–	81.26	6.72	0.43	1.90	3.82
N1	1:2	1	27	91.20	3.58	0.17	0.70	0.00
N2	1:4	1.5	47	92.04	3.85	0.20	0.74	0.00
N3	1:4	1	50	92.51	3.77	0.21	0.73	–
N4	1:5	3	50	91.42	3.63	0.13	0.64	0.13

Table 2
Main textural characteristics of the carbons

Carbon	N0	N1	N2	N3	N4
W_o ($cm^3\ g^{-1}$)	0.35	0.75	0.91	0.96	1.03
E_o ($kJ\ mol^{-1}$)	21.57	20.92	19.45	19.34	18.84
L_o (nm)	1.06	1.13	1.34	1.36	1.45
S_{mi} ($m^2\ g^{-1}$)	659	1327	1356	1406	1421
S_e ($m^2\ g^{-1}$)	17	23	30	64	50
$TSA = S_{mi} + S_e$ ($m^2\ g^{-1}$)	676	1350	1386	1470	1471
S_{comp} ($m^2\ g^{-1}$)	569	1256	1406	1424	1563
S_{phenol} ($m^2\ g^{-1}$)	595	1277	1413	1330	1516
$S_{total} = [TSA + S_{comp} + S_{phenol}]/3$ ($m^2\ g^{-1}$)	613	1294	1450	1408	1517
S_{BET} ($m^2\ g^{-1}$)	835	1901	2400	2522	2800
$-\Delta_i H[C_6H_6, 0.41\ nm]$ ($J\ g^{-1}$)	100.5	220.9	254.1	232.5	266.3
$-\Delta_i H[C_6H_{12}, 0.54\ nm]$ ($J\ g^{-1}$)	70.7	–	–	–	–
$-\Delta_i H[CCl_4, 0.63\ nm]$ ($J\ g^{-1}$)	70.3	–	–	–	–
$-\Delta_i H[CDDT, 0.76\ nm]$ ($J\ g^{-1}$)	62.2	218.8	251.0	223.7	274.0
$-\Delta_i H[TXP, 1.50\ nm]$ ($J\ g^{-1}$)	53.8	211.4	260.7	226.2	270.1

(PVDF Kynar Flex 2801) and 5 wt.% of acetylene black. Electrodes were prepared in the form of pressed pellets (7–10 mg) with a geometric surface area of 0.8 cm^2 per electrode. Electrochemical investigations were performed in acidic (1M H_2SO_4), alkaline (6M KOH) and organic (1M tetraethyl ammonium tetrafluoroborate in acetonitrile, $(C_2H_5)_4NBF_4$/AN) electrolytic solutions. A glassy fibrous material played the role of separator. The capacitance properties of the composite materials (expressed per active mass of a single electrode) were studied by galvanostatic (50–20,000 mA g^{-1}), potentiodynamic cycling at voltage scan rates from 1 to 100 mV s^{-1}, and by impedance spectroscopy (100–1 mHz) using VMP2/Z Biologic, France and AUTOLAB 30 FRA2-Netherlands potentiostat-galvanostats.

3. Results and discussion

3.1. Porous structure of the activated carbons

The results of the adsorption and immersion experiments for carbons N0–N4 are summarized in Table 2.

The Dubinin–Radushkevich (D–R) plot for N_2 adsorbed on carbon N0 leads to a micropore volume $W_o = 0.35\ cm^3\ g^{-1}$ and a characteristic energy E_o, of 21.6 $kJ\ mol^{-1}$, which corresponds to an average micropore width $L_o = 1.06$ nm [12]. For slit-shaped micropores the surface area of the walls S_{mi} ($m^2\ g^{-1}$) = $2000 W_o$ ($cm^3\ g^{-1}$)/L_o (nm), and consequently the micropore system of N0 probed by N_2 has a specific surface area of 659 $m^2\ g^{-1}$. On the other hand, the comparison with a non-porous carbon leads to an external (non-microporous) surface area S_e of 17 $m^2\ g^{-1}$ and also confirms the value of the micropore volume obtained from the DR plot. Furthermore, the data for E_o, W_o and S_e has been cross-checked by the enthalpy of immersion into C_6H_6 at 293 K. The calculated [12–13] and the experimental values of $-\Delta_i H(C_6H_6)$ for N0 are, respectively, 100.5 and 104.7 $J\ g^{-1}$. The good agreement indicates that both molecules probe the same micropore volume and confirms self-consistency between the adsorption and immersion data.

Back-calculations based on the experimental enthalpies of immersion of N0 into a series of liquids with critical dimensions L_c between 0.33 nm (CH_2Cl_2) and 1.5 nm (TXP) lead to the micropore volumes $W(L_c)$ filled by these molecular probes (Fig. 1). Immersion calorimetry suggests that most micropores of the commercial activated carbon are smaller than 0.6 nm whereas the average micropore size estimated from the adsorption of nitrogen and the immersion into benzene corresponds to 1.06 nm. This disagreement is, in fact, a direct consequence of so-called 'gate' or molecular-sieve effects due to constrictions of approximately 0.6 nm at the entrance of the pore system, which reduce the accessibility of molecules normally compatible with the actual internal micropore sizes [15].

As reported in Table 2, the specific surface areas estimated from the enthalpy of immersion into phenol (S_{phenol}) and from the comparison plot (S_{comp}) are in relatively good agreement with the total surface area derived from $TSA = S_{mi} + S_e$. The combination of these approaches allowed estimating an average total surface area (S_{total}) of 613 $m^2\ g^{-1}$ for the commercial activated carbon N0.

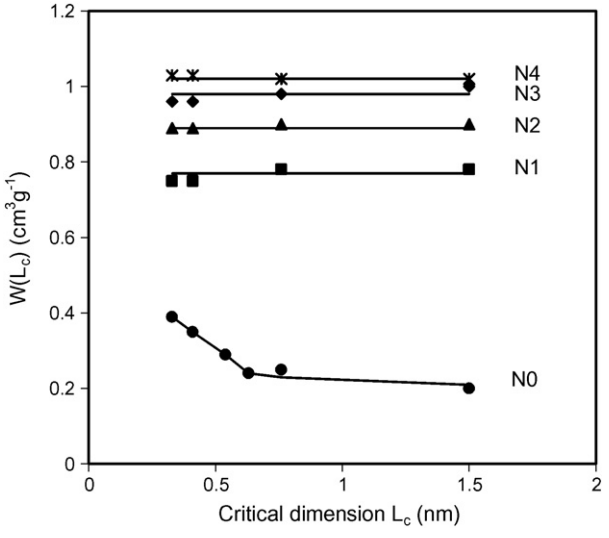

Fig. 1. Micropore volume of activated carbons accessible to liquids with different molecular sizes.

A first indication of the effect of KOH-treatment on the original structure of N0 is provided by the adsorption characteristics of the materials N1–N4, summarized in Table 2. The micropore volume W_o increases significantly with mild activation and a volume of 0.75 $cm^3\,g^{-1}$ is already achieved at 27% burn-off (carbon N1) against 0.35 $cm^3\,g^{-1}$ for the original carbon. The change in the microporous network is also indicated by the increase in the enthalpies of immersion into the molecular probes (Table 2). As illustrated by Fig. 1, the micropore system of N1 is equally accessible to molecules of different sizes although the average micropore size is only slightly larger (1.13 nm) than in carbon N0 (1.06 nm). That means that up to 27% burn-off, the changes affect mainly the constrictions, rather than the internal pore size. Further activation up to 50% burn-off (carbons N2–N4) develops the internal micropore system and leads to micropore volumes around 1.0 $cm^3\,g^{-1}$ and to average widths L_o of 1.3–1.4 nm. A similar pattern has been observed earlier for carbons with 'gate' effects [15]. For our materials, the gradient $\Delta L_o/\Delta W_o$ is approximately 0.52 nm/(cm^3/g), independently of the activation conditions.

As reported in Table 2, the effective surface areas of the re-activated materials (determined from the average value of the surface area obtained from the three independent techniques, $S_{total} = (TSA + S_{comp} + S_{phenol})/3$ are in the range 1300–1500 $m^2\,g^{-1}$. Therefore, they exceed the values obtained for many activated carbons typically between 700 and 1000 $m^2\,g^{-1}$. They can be compared favourably with the upper-bounds found for the specific surface area of mesoporous carbons obtained by the so-called templating technique (1500–1600 $m^2\,g^{-1}$) [16].

Table 2 also shows that the BET surface areas for the re-activated carbons do not agree with the other determinations and the values can be as high as 2800 $m^2\,g^{-1}$ (in fact, these values are the monolayer equivalents of W_o [13] and this is due to the presence of a large proportion of supermicropores in carbons N1–N4). In the present study, S_{BET} leads clearly to erroneous surface related capacitances and consequently our interpretation of the electrochemical properties is based on $S_{total} = (TSA + S_{comp} + S_{phenol})/3$, in order to establish reliable surface-related correlations [8,14,16].

3.2. *Electrochemical properties of the activated carbons*

The KOH activation of the commercial activated carbon N0 leads to a remarkable increase in the electrochemical capacitance. As reported in Table 3, specific capacitances up to 200 $F\,g^{-1}$ in aqueous electrolytes and around 150 $F\,g^{-1}$ in 1M $(C_2H_5)_4NBF_4$/AN are achieved by re-activated carbons N1–N4.

In the case of the aqueous electrolytes, the comparison between the sets of data for 1M H_2SO_4 and 6M KOH indicates similar trends for the performance of carbons N0–N4 in both media (Table 3). Fig. 2 compares the gravimetric specific capacitance at 50 $mA\,g^{-1}$ measured in H_2SO_4, $C_{50\text{-acidic}}$, with the total specific surface area S_{total} of all carbons. It can be seen that N0 fits to the general pattern found for standard activated carbons with total surface areas around 500–700 $m^2\,g^{-1}$, the specific surface related-capacitance ($C_{50\text{-acidic}}/S_{total}$) being

Table 3
Specific capacitances ($F\,g^{-1}$) estimated by three electrochemical methods for the commercial activated carbon N0 and the re-activated carbons N1–N4

	Carbon N0			Carbon N1			Carbon N2			Carbon N3			Carbon N4		
	H_2SO_4 ($F\,g^{-1}$)	KOH ($F\,g^{-1}$)	$(C_2H_5)_4NBF_4$ ($F\,g^{-1}$)	H_2SO_4 ($F\,g^{-1}$)	KOH ($F\,g^{-1}$)	$(C_2H_5)_4NBF_4$ ($F\,g^{-1}$)	H_2SO_4 ($F\,g^{-1}$)	KOH ($F\,g^{-1}$)	$(C_2H_5)_4NBF_4$ ($F\,g^{-1}$)	H_2SO_4 ($F\,g^{-1}$)	KOH ($F\,g^{-1}$)	$(C_2H_5)_4NBF_4$ ($F\,g^{-1}$)	H_2SO_4 ($F\,g^{-1}$)	KOH ($F\,g^{-1}$)	$(C_2H_5)_4NBF_4$ ($F\,g^{-1}$)
Cyclic voltammetry at different scan rates ($mV\,s^{-1}$)															
1	95	97	50	168	170	126	176	186	135	160	176	138	202	180	150
2	89	95	48	157	164	122	164	178	133	153	162	128	190	175	147
5	85	93	45	152	159	116	157	174	128	142	158	126	174	169	145
10	82	90	43	147	155	111	153	169	122	139	152	120	162	166	140
20	77	86	40	142	148	107	150	160	117	136	146	116	149	155	134
50	70	75	35	134	137	103	142	143	104	129	130	107	136	124	126
100	62	68	32	125	122	94	133	129	92	126	116	91	109	92	119
Impedance (1 mHz)	89	81	34	160	157	113	176	172	125	141	140	115	170	162	125
Cycle number (500 $mA\,g^{-1}$)															
1	91	86	40	153	155	118	162	170	129	139	144	118	157	166	141
1000	91	79	39	159	144	113	170	163	123	137	139	116	149	162	136
2000	91	79	40	158	139	112	169	158	121	135	135	112	142	158	133
3000	90	80	39	158	134	110	168	152	119	135	133	109	134	155	130
4000	90	78	39	158	130	109	168	143	117	133	130	108	126	151	126
5000	89	77	39	157	127	108	167	137	115	132	128	106	118	149	123

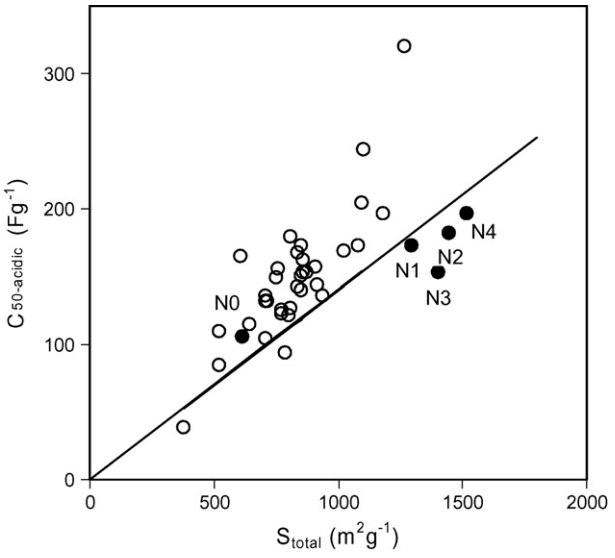

Fig. 2. Variation of the specific capacitance at 50 mA g^{-1} in acidic electrolyte, $C_{50\text{-acidic}}$, with the total surface area of carbons of Table 2 (●) and typical activated carbons from Refs. [7,8,10] (◯). The line through the origin corresponds to a linear best fit for carbons with low oxygen and ash contents (mesoporous templated carbons) [16].

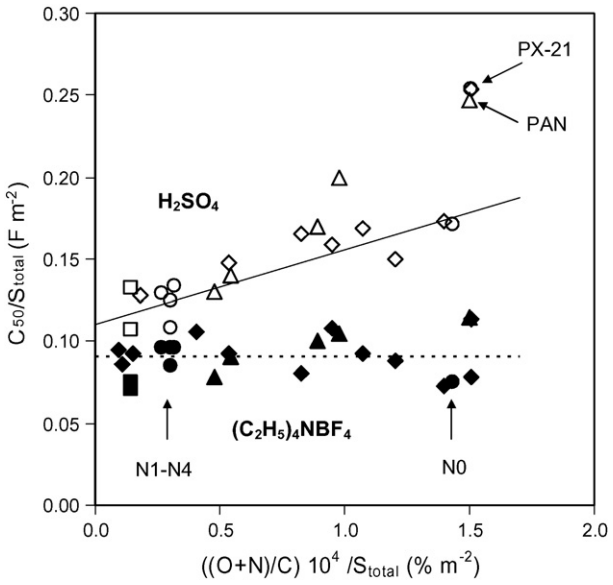

Fig. 3. Variation of the surface-related capacitances at 50 mA g^{-1}, C_{50}/S_{total}, with the density of oxygen and nitrogen ((O + N)/C)/S_{total} for different carbons in the acidic (open symbols) and organic electrolytes (closed symbols): present work (◯), typical activated carbons [7,8,10] (◊), activated carbons from *N*-polymers [9] (△) and templated mesoporous carbons [11] (□).

approximately 0.17 F m^{-2}. This value for the re-activated carbons drops to 0.124 F m^{-2}, as opposed to 0.250–0.260 F m^{-2} obtained for certain activated carbons with similar S_{total} [8]. On the other hand, the contribution provided by N1–N4 is in good agreement with the correlation of 0.13–0.14 F m^{-2} found for carbons with low oxygen and ash contents, such as mesoporous templated carbons [11,16].

Table 1 suggests that the changes induced in carbon N0 by the KOH-treatment are not exclusively due to the porous structure and that the purity of the carbons is notably enhanced by ash removal. Furthermore, a marked reduction in the total amount of oxygen and nitrogen also takes place during the activation process. One may therefore assume that it leads to a smaller density of surface functionalities in carbons N1–N4, which significantly affects their electrochemical properties. As shown recently [5,8,9], certain oxygen- and nitrogen-surface complexes have a positive contribution to the overall capacitance at low and medium current density in the form of quick redox reactions (pseudo-capacitance), to be added to the purely double layer capacitance associated with the surface area.

Fig. 3 shows the variation of the specific capacitances $C_{50\text{-acidic}}/S_{total}$ with the surface density of oxygen and nitrogen ((O + N)/C)/S_{tot} for different carbons, including limiting cases such as PX-21 (a KOH-activated carbon with a total oxygen content of 9.4 mmol g^{-1} or 7.4 μmol m^{-2}) and PAN (a polyacrylonitrile derived-activated carbon with a total nitrogen content of 7.2 wt.%).

Although the influence of the different surface complexes would require a detailed analysis, a significant decrease in the surface-related capacitance is observed for carbons N1–N4 in H_2SO_4, whereas their gravimetric capacitance is twice of that of the raw carbon. It seems that the performance of the re-activated carbons in H_2SO_4 arises essentially from the double layer capacitance formed on their surface and, therefore, this behaviour compares with that of novel materials such as mesoporous templated carbons [11,16].

Since the energy of an electrochemical capacitor increases with the square of the operating voltage, a substantial improvement of this parameter can be achieved by using non-aqueous electrolytes with higher decomposition voltage than that of aqueous electrolytes. However, as already reported [10], the specific capacitance of typical activated carbons (S_{total} between 700 and 1000 m^2 g^{-1}) rarely exceeds 100 F g^{-1} in the aprotic electrolytes at low current densities.

Table 3 reports the excellent performance of carbons N1–N4 in the aprotic electrolyte 1M $(C_2H_5)_4NBF_4$/AN, where values as high as 150 F g^{-1} are achieved. Hence, for the best sample N4, the specific energy of 20 W h/kg (calculated per mass of both electrodes) can be reached.

The effective surface areas in the range 1300–1500 m^2 g^{-1} obtained by KOH treatment of N0 result in gravimetric capacitances almost three times higher than that of the raw carbon (S_{total} = 613 m^2 g^{-1}). As illustrated by Fig. 4, the materials of the present work follow the profile observed for typical activated carbons in $(C_2H_5)_4NBF_4$/AN at low current density [8,9]. They also surpass the behaviour of templated mesoporous carbons with similar specific surface areas [11,16]. Fig. 3 shows that the pseudocapacitive effects are not significant in the aprotic electrolyte and the double layer contribution is limited to 0.08–0.09 F m^{-2} in 1M $(C_2H_5)_4NBF_4$/AN.

Further details on the different properties of re-activated carbons N1–N4 compared to those of typical activated carbons are provided by experiments based on immersion calorimetry. The analysis of the correlation between the specific capacitance at 50 mA g^{-1} and the enthalpy of immersion into benzene at 293 K

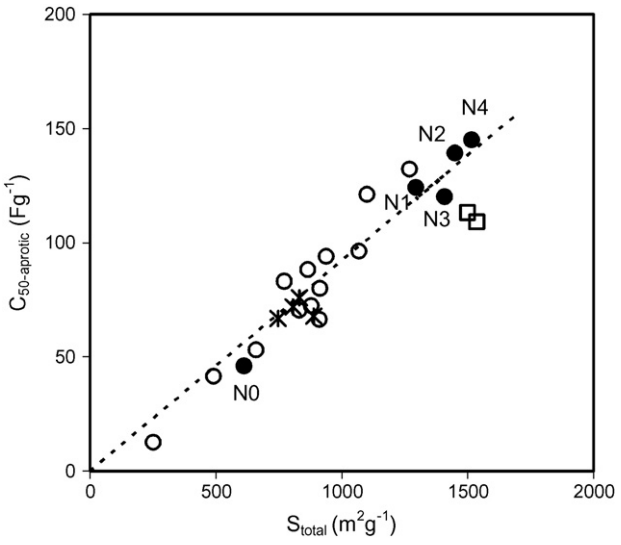

Fig. 4. Variation of the specific capacitance at 50 mA g^{-1} in organic electrolyte, $C_{50\text{-aprotic}}$, with the total surface area of carbons of Table 2 (●), typical activated carbons [8] (◯), activated carbons from *N*-polymers [9] (*) and templated mesoporous carbons [11] (□). The line through the origin corresponds to the linear best fit for activated carbons.

(Fig. 5) indicates that in the case of the acidic electrolyte, the contribution of the present carbons is well below the average value around $-1.1\,\mathrm{F\,J^{-1}}$ observed for a large variety of activated carbons [7]. As shown recently [8,14], this value reflects the role of the active surface area (ASA) which tends to increase with the micropore volume W_o of carbons obtained by standard activation processes, according to the correlation ASA (m^2 g^{-1}) = 166 (m^2 cm^{-3})W_o (cm^3 g^{-1}) suggested earlier [17]. The deviation observed for carbons N1–N4 is a consequence of the specific procedure for their preparation.

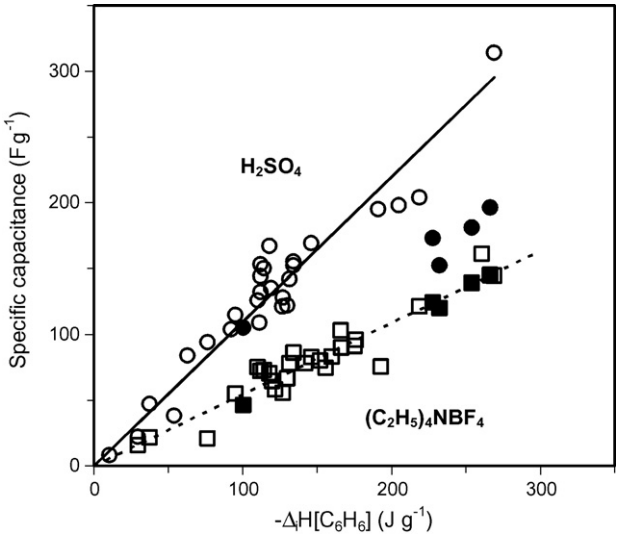

Fig. 5. Correlation between the specific capacitance at low current density (50 mA g^{-1}) of different activated carbons and the enthalpy of immersion into benzene. In H_2SO_4: carbons of the present study (●) and typical activated carbons [7,8,10] (◯). In $(C_2H_5)_4NBF_4$/AN: carbons of the present study (■) and typical activated carbons [7,8,10] (□).

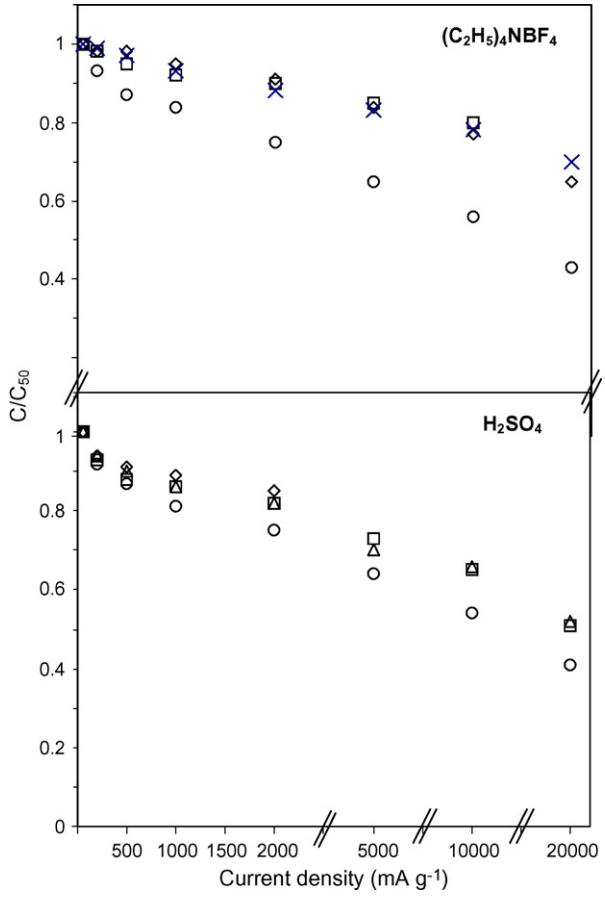

Fig. 6. Variation of the relative capacitance C/C_{50} with the current density for carbons N0 (◯), N1 (□), N2 (△), N3 (◊) and N4 (X) in aqueous and aprotic electrolytes.

On the other hand, it is interesting to note that the values of the capacitance in the aprotic electrolyte follow the earlier empirical correlation of $-0.544\,\mathrm{F\,J^{-1}}$ (Fig. 5). This confirms the weak effects of the surface functional groups on $C_{50\text{-aprotic}}$ as far as the enthalpy of immersion into benzene $-\Delta_i H(C_6H_6)$ does not depend on the chemical nature of carbon surface [12].

The present study confirms the possibility offered by immersion calorimetry for the prediction of the specific capacitance of unknown carbons in organic electrolyte, *e.g.* $(C_2H_5)_4NBF_4$/AN. On the other hand, it also shows the limitations of this technique to assess, with a good accuracy, the suitability of a carbon to be used in aqueous H_2SO_4 capacitors, where oxygen-containing surface complexes also play a role. These complexes have no influence on $-\Delta_i H(C_6H_6)$.

It is observed that the KOH-treatment does not only increase the capacitance of carbons at low current density, but also provides promising materials with good performance at high current densities. This is illustrated by Fig. 6, which compares the evolution of normalized capacitance C/C_{50} with current density in the $(C_2H_5)_4NBF_4$/AN and H_2SO_4 electrolytes. The slower decrease of C observed in the aprotic electrolyte for the reactivated carbons indicates that such materials present a more accessible porous structure than usually found in the standard activated carbon N0. Even for burn-off around 27%, sample

N1 still delivers at 10,000 mA g^{-1} around 80% of the capacitance achieved at 50 mA g^{-1}. As seen in Fig. 6, the ratios C/C_{50} are similar for carbons N1–N4, independently of the internal micropore dimension, which suggests that the mobility of the $(C_2H_5)_4N^+$ ion (0.69 nm) is affected by the constrictions of approximately 0.6 nm observed for the initial carbon N0. The present study shows that the removal of the "gate" effect by KOH-treatment leads to carbons with a porous structure well adapted to high charge/discharge loads in $(C_2H_5)_4NBF_4$/AN medium. These carbons also surpass the behaviour reported for a variety of mesoporous carbons with pore sizes up to 10 nm [11,16].

In the case of the H_2SO_4 electrolyte, constrictions near 0.6 nm do not affect significantly the mobility of the solvated sulfate ion (0.53 nm) and, according to previous studies [8], the somewhat better performance observed in the H_2SO_4 aqueous electrolyte for re-activated carbons should be ascribed to their lower total oxygen content rather than differences in structural properties. This is an advantage over most activated carbons, which contain more acidic groups.

For the potential use of a given carbon as a capacitor electrode, one must consider very carefully its ability to withstand long-term cycling. Table 3 shows that the capacitance values of carbons N1–N4 decrease slightly after cycling at a current density of 500 mA g^{-1}. It has been reported that some surface functionalities tend to disappear with charge/discharge cycles and a corresponding loss in the overall capacitance of the supercapacitor is observed [4]. As a result of their high purity, the performance of the present carbons seems to be essentially based on a double layer mechanism which ensures an enhanced and stable capacitance.

4. Conclusions

The present study shows that materials with superior properties for electric double-layer capacitors can be produced by a simple treatment of an inexpensive activated carbon with KOH at 850 °C. The improvement of EDLC performance is attributed to the changes produced by this secondary activation on the porous structure, as well as on the chemical characteristics of the commercial carbon.

The effective surface areas for the re-activated materials are in the range of 1300–1500 m^2 g^{-1} and, therefore, exceed the values obtained for typical activated carbons usually in the range 700–1000 m^2 g^{-1}. Simultaneously, one observes a marked increase in the purity of carbons.

KOH-treatment leads to specific capacitances up to three times higher than that of the raw carbon. Values of 200 F g^{-1} in aqueous electrolytes (1M H_2SO_4 and 6M KOH) and around 150 F g^{-1} in 1M $(C_2H_5)_4NBF_4$ in acetonitrile are achieved by re-activated carbons at low current density (50 mA g^{-1}). Furthermore, the resulting carbons present an enhanced performance for high charge/discharge load in organic and aqueous media.

It has been reported that typical activated carbons usually present a pseudocapacitive contribution from surface functionalities which tend to disappear with capacitor cycling, producing a loss in the overall capacitance. As a result of their high purity, the performance of the present carbons is essentially based on a double layer mechanism which ensures a stable capacitance.

The present study also confirms the possibilities offered by immersion calorimetry for the prediction of the specific capacitance of carbons in organic medium, *e.g.* $(C_2H_5)_4NBF_4$/AN. On the other hand, there may be limitations of capacitance estimation in the case of aqueous electrolytes if the carbons contain important amounts of surface oxygen. The latter plays a role in the pseudocapacitance, but it is practically not detected by immersion into benzene, as shown by experiments with carbons containing various amounts of oxygen.

Acknowledgement

The support from the Programme for Scientific and Technological Cooperation Spain-Poland is highly acknowledged.

References

[1] A. Burke, J. Power Sources 91 (2000) 37.
[2] R. Kötz, M. Carlen, Electrochim. Acta 45 (2000) 2483.
[3] A. Burke, Electrochim. Acta (2007), in press.
[4] A.G. Pandolfo, A.F. Hollenkamp, J. Power Sources 157 (2006) 11.
[5] M.J. Bleda-Martínez, J.A. Maciá-Agulló, D. Lozano-Castelló, E. Morallón, D. Cazorla-Amorós, A. Linares-Solano, Carbon 43 (2005) 2677.
[6] M.J. Bleda-Martínez, D. Lozano-Castelló, E. Morallón, D. Cazorla-Amorós, A. Linares-Solano, Carbon 44 (2006) 2642.
[7] T.A. Centeno, F. Stoeckli, J. Power Sources 154 (2006) 314.
[8] T.A. Centeno, F. Stoeckli, Electrochim. Acta 52 (2006) 560.
[9] E. Frackowiak, G. Lota, J. Machnikowski, C. Vix-Guterl, F. Béguin, Electrochim. Acta 51 (2006) 2209.
[10] T.A. Centeno, M. Hahn, J.A. Fernández, R. Kötz, F. Stoeckli, Electrochem. Comm. 9 (2007) 1242.
[11] A.B. Fuertes, G. Lota, T.A. Centeno, E. Frackowiak, Electrochim. Acta 50 (2005) 2799.
[12] F. Stoeckli, Characterization of microporous carbons by adsorption and immersion techniques, in: J. Patrick (Ed.), Porosity in Carbons-Characterization and Applications, Arnold, London, 1995, p. 67.
[13] F. Stoeckli, T.A. Centeno, Carbon 43 (2005) 1184.
[14] T.A. Centeno, F. Stoeckli, Structural and chemical characterization of carbons used as supercapacitors, in: V. Gupta (Ed.), Recent Advances in Supercapacitors, Transworld Research Network, Kerala, 2006, p. 57.
[15] F. Stoeckli, A. Slasli, D. Hugi-Cleary, A. Guillot, Micropor. Mesop. Mat. 51 (2002) 197.
[16] M. Sevilla, S. Alvarez, T.A. Centeno, A.B. Fuertes, F. Stoeckli, Electrochim. Acta 52 (2007) 3207.
[17] P. Ehrburger, N. Pusset, P. Dziedzinl, Carbon 30 (1992) 1105.